Lead-cooled fast reactor SMR integration: An off-grid study case based on a real-life demand

Antoine Larbanois[a,*], Bardhyl Miftari[a], Antoine Mouchamps[a], Ayyildiz Kerem Enes[b], Vincent Schryvers[b], Guillaume Derval[a], Damien Ernst[a]

[a]*Department of Computer Science and Electrical Engineering, Liège University, Liège, Belgium*
[b]*SCK-CEN, Belgian Nuclear Research Centre, Mol, Belgium*

Abstract

This paper analyses the integration of a specific type Small Modular Reactor (SMR), namely a Lead-cooled Fast Reactor (LFR), along with storage and conversion units, to power an off-grid, energy-intensive industrial site, with both heat and electricity demands.

Despite the partial load-following capability of the LFR-SMR and its integration with a thermal energy unit, significant seasonal fluctuations in industrial energy demand make the LFR-SMR alone inappropriate to ensure continuous year-round supply adequacy. To address this limitation, additional storage and energy conversion units are required.

Accordingly, we evaluate the technical and economic performance of three configurations designed to meet the combined heat and electricity demands over the full year. The first incorporates a lithium-ion battery; the second integrates hydrogen production and storage; and the third builds upon the second by also incorporating ammonia as an additional energy carrier. Each configuration is optimally sized and operated to minimise system cost.

Our results show that an LFR-SMR can operate off-grid in all configurations. The reactor, along with its thermal storage, effectively manages minor fluctuations in energy demand, while the conversion and storage units are primarily used during peak consumption periods that exceed the reactor's maximum output. Solutions based on synthetic fuels prove to be significantly more cost-effective than the battery-based approach, with a slight advantage for the ammonia-based configuration. For the latter, we estimate the heat cost of €25/MWh and an electricity cost of €59/MWh. The additional units enabling off-grid operation represent less than 4% of the total cost.

Keywords: SMR, Nuclear, Hydrogen, LFR, Optimisation of energy systems, Off-grid

1. Introduction

European countries face significant challenges in their aim to decarbonise their economy while simultaneously providing affordable energy to their households and ensuring security of supply. For example, in Belgium, despite the promising future of renewable energy sources, numerous studies indicate that their integration potential is limited to less than 100 TWh per year [1, 2], whereas the national final energy consumption is predicted to be around 400 TWh in 2050 [2].

In this context, nuclear energy emerges as a promising source of reliable low-carbon energy. In particular, the Belgian government has expressed interest in Small Modular Reactors (SMR) [3], prompting the Belgian Nuclear Research Centre (SCK-CEN) to investigate the development and deployment of a particular type of SMR known as Lead-cooled Fast Reactor (LFR).

SMRs offer numerous advantages over larger, traditional nuclear reactors. Their smaller size reduces construction costs by allowing their components to be manufactured in factories and then transported to their installation site [4]. In some cases, SMRs integrate passive cooling systems as part of their safety design, allowing them to operate independently of external power sources [5]. They also have the ability to use the heat generated for industrial processes or residential heating systems [6].

LFRs, which sustain nuclear reactions through fast neutrons and which use molten lead as a primary coolant, present additional benefits. They can operate at high temperatures up to 500 °C, which enables applications in high-temperature industrial processes and hydrogen production [7], and allows for higher thermal efficiencies [8]. They also produce significantly less radioactive waste, thanks to fast neutrons chain reactions, which also enable the possibility to recycle some of this nuclear waste as fuel, such as the plutonium in Mixed Oxide (MOX) fuels [9, 10].

In this paper, we study the implementation of an LFR-SMR in an off-grid scenario. There are two main reasons for studying the off-grid setting. First, regarding security of supply, with the increasing deployment of intermittent renewable energy sources, coupled with growing geopolitical tensions affecting energy supply, modern energy grids are becoming more susceptible to disruptions [11, 12]. In this context, an off-grid SMR could offer a reliable and independent source of heat and electricity, ensuring energy continuity even in the face of major disruptions. Second, given the uncertainty surrounding

*Corresponding author
Email address: antoine.larbanois@uliege.be (Antoine Larbanois)

the grid's capacity to integrate multiple SMRs (whose power can reach up to 714 MWth – 300 MWe), examining an off-grid configuration allows us to bypass the externalities and constraints typically associated with connection to the grid. Additionally, this case study enables the estimation of an upper bound on the cost of heat and electricity for an SMR-industry system connected to the grid, as the connection would be implemented only if it leads to lower costs.

To assess the capability of an SMR to operate off-grid, we study a specific case: a 714 MWth reactor (300 MWe) coupled with a 4,000 tonne molten salt thermal storage unit and a cooling tower, supplying an energy-intensive industrial site with a primary annual demand of 4,000 GWh, in the form of electricity and heat, that must be satisfied at all times. The primary demand cannot be met by the SMR and its thermal storage alone due to peak moments exceeding the reactor's maximum capacity and moments where demand falls below its minimum operational threshold. Expanding the reactor's size would lead to a lower capacity factor, adversely affecting cost-effectiveness. We thus, integrate additional technologies that can be used as storage and conversion units for coping with potential excess production or production deficit. These additional units can be seen as a secondary flexible demand for heat and electricity, as illustrated in Figure 1. When releasing stored energy, they also function as a secondary source of production.

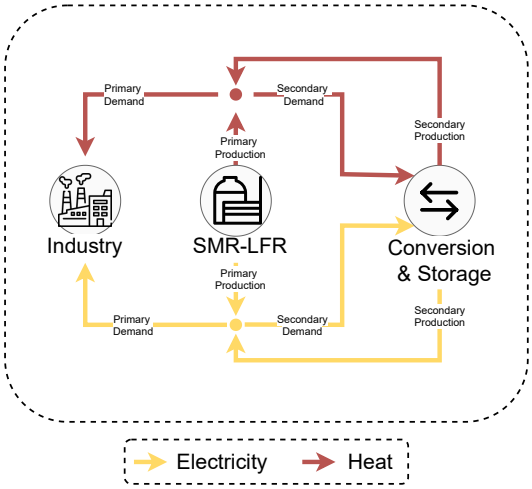

Figure 1: Diagram of the primary and secondary demand and production flows.

We study three configurations. The first relies on a battery system to ensure energy autonomy. The second combines batteries with hydrogen production and storage facilities, which can also provide a secondary heat source through combustion in a dedicated burner. The third configuration goes further by integrating ammonia, synthesised from hydrogen and nitrogen. It includes batteries and storage systems for both hydrogen and ammonia, along with a hybrid burner capable of using both gases to deliver an additional source of heat.

This article is structured as follows. In Section 2, we discuss the related work. Section 3 defines the scope of the analysis and Section 4 presents the different configurations studied. Afterwards, in Section 5 we describe the methodology and underlying assumptions used in our study. The results are then presented and discussed in Section 6. As part of these results, we also report on a sensitivity analysis on technical and economic parameters of the LFR-SMR, as well as on the choice of electrolysers. Finally, Section 7 concludes the paper and gives directions for future research.

2. Related works

The literature on Small Modular Reactors (SMRs) in off-grid configurations is covered by various research areas. Indeed, SMRs have been, for example, the subject of market studies, conceptual reactor designs, and demand-side flexibility strategies. Another research area, more related to our work, explores the economic feasibility of deploying SMRs in industrial applications. In this section, we review the existing literature in these areas, identify some gaps, and demonstrate how our study addresses these shortcomings.

Regarding off-grid scenarios, Wojtaszek and Tadeusz [13] analyse the Canadian market for off-grid applications such as mining operations, oil and gas extraction facilities, and remote communities. While this study provides valuable insights from a market perspective, it lacks a detailed assessment of the technical and operational feasibility of SMR deployment in such environments. Wallenius et al. [14] present the conceptual design of a small-scale, lead-cooled nuclear reactor with an electric output of 3 MWe. The proposed system aims to replace diesel generators in off-grid applications located in remote regions. A number of studies have focused on SMRs operating at constant output while achieving overall system flexibility through demand-side technologies. For instance, Locatelli et al. [15], Locatelli et al. [16], and Ma et al. [17] explore systems where flexibility is introduced via secondary applications such as hydrogen production, desalination, district heating, or other industrial processes. In these works, SMRs are not used for load following; instead, excess energy is absorbed by flexible secondary demand, demonstrating a viable path for integrating nuclear energy into multi-vector energy systems.

In terms of economic feasibility, Locatelli et al. [7] assess various industrial uses of SMRs and identify industrial heating, hydrogen production, and desalination as the most promising applications. Further supporting this, Locatelli et al. [15] confirm the viability of hydrogen production, while Ashoori and Gates [18] demonstrate the profitability of SMRs for oil sands extraction. Both studies employ Discounted Cash Flow (DCF) analysis to evaluate the financial viability of these applications. These studies highlight that the profitability of cogeneration in SMRs is highly project specific, depending on both the technical and economic characteristics of the selected reactor, as well as on the regulatory framework, as confirmed in Van Hee et al. [19].

Despite the growing body of work, current literature does not examine a specific off-grid industrial case with real-life data where the SMR production can be modulated in addition to the secondary flexible demand. Our work aims to address this gap by developing models that assess both the technological requirements and the economic feasibility of a lead-cooled fast reactor operating with additional technologies to support off-grid operation.

3. Problem statement

In this paper, we investigate the technical and economic performance of deploying an SMR to meet the primary demands of a large-scale chemical plant in an off-grid configuration. Specifically, we analyse the integration of a 714 MWth (300 MWe) LFR coupled with a 4,000 ton molten salt thermal storage unit and a cooling tower, a design under study by the Belgian Nuclear Research Centre [20], to supply both heat and electricity for an industrial site with an annual final energy demand of 4,000 GWh. The majority, 85%, is for heat, while the remaining 15% is for electricity.

This study uses a real, fixed industrial demand profile, ensuring that the analysis accurately reflects actual operational constraints. The demand profile includes periods during which reliance on a secondary energy source is essential to guarantee a continuous supply. Indeed, at certain times, demand peaks exceed the maximum capacity of the reactor, making it necessary to add an additional heat or electricity source. The plant is assumed to be entirely energy independent, with no exchange of electricity or heat with external grids.

We consider an operational framework in which the LFR-SMR is capable of modulating its output while integrating thermal energy storage to enhance its flexibility in response to the plant's real-time energy demand. Additionally, the LFR-SMR system relies on storage and conversion units, including lithium-ion batteries and synthetic energy carriers such as hydrogen and ammonia, to store part of its production. During periods of low demand, surplus energy is either stored in batteries or used for the production of synthetic fuels. When the reactor output is insufficient to meet instantaneous energy requirements, the stored energy is converted and dispatched as secondary production to compensate for the deficit.

To estimate the required capacities of the various units considered in this study, an optimisation process is carried out to determine their optimal sizing and operational strategy in order to meet the industrial energy demand. The capacities of the LFR-SMR and its thermal storage are assumed to be fixed.

4. Case studies

As previously mentioned, the LFR-SMR by itself cannot follow the demand curve, additional solutions are necessary to maintain a continuous energy supply. This section introduces a selection of technologies that can be used to fulfil this continuity requirement.

We analyse three distinct energy storage and conversion configurations. The first one relies on lithium-ion batteries, providing a secondary source of electricity for the industry. The second expands on the first configuration by incorporating hydrogen production. In addition to the battery system, it includes a solid oxide electrolyser cell (SOEC) for hydrogen generation, a hydrogen storage unit, and a burner to supply supplementary heat. The third configuration integrates ammonia synthesis via a Haber-Bosch unit, which is fuelled by hydrogen and nitrogen produced through the SOEC electrolyser. This configuration also features ammonia storage, and its burner can combust a mixture of hydrogen and ammonia to deliver an additional heat source to the industry. These configurations, along with the associated technologies, are discussed in detail in the subsections below. However, we first introduce, at this point, the two units common to all configurations, namely the LFR-SMR and the industrial system.

The LFR-SMR considered has, as previously indicated, a thermal capacity of 714 MWth and an electrical output of 300 MWe. As illustrated in Figure 2, the LFR-SMR incorporates several subsystems: the reactor core, a thermal storage, a steam turbine, and a cooling tower. The system is structured around two main thermal circuits that enable a stepwise heat transfer process. The primary circuit (composed of liquid lead) extracts heat from the reactor core, which uses MOX fuel, and transports this heat to the thermal storage unit. The secondary circuit (composed of molten salt), also called the thermal storage, supplies heat to the steam turbine and delivers high-quality heat to meet industrial demand. The cooling tower is used to reject both high-grade heat that is unused from the secondary circuit and low-grade residual heat discharged from the steam turbine. The electricity generated is used to meet the power demand, charge batteries, and supply energy to electrolysers. The reactor design includes 2,000 tonnes of lead in the primary circuit and 4,000 tonnes of molten salt in the secondary circuit. This configuration enables a more flexible allocation of thermal energy between the demands of heat and electricity. It directly reflects the design studied by SCK-CEN and is considered fixed; therefore, it is not subject to optimisation in this paper.

For the industry, we use the real-life energy demand from a chemical industrial plant in Belgium for electricity and heat throughout the year with a fifteen-minute resolution. These energy demand profiles were provided by the Belgian gas and electricity TSOs. The annual energy demand for the plant is 4,000 GWh, of which approximately 15% is dedicated to

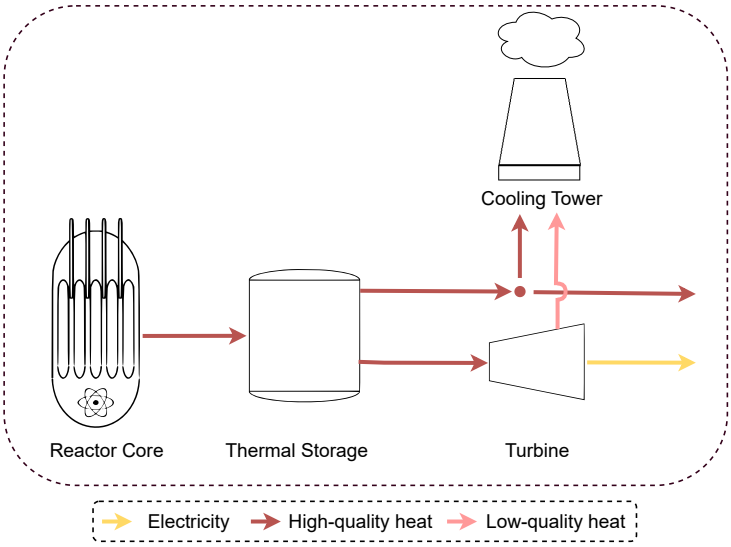

Figure 2: Configuration of the LFR-SMR, including the reactor core, thermal storage, cooling tower, and the turbine. The energy system transforms the primary energy generated by the reactor core into two energy vectors: electricity and heat.

electricity demand, while the remainder 85% is used for heat. A representation of the total heat demand (heat used directly in industry and the equivalent heat needed to cover electricity demand) is shown in Figure 6. The demand curves present two interesting characteristics: first, several consecutive days during which the demand exceeds the reactor's maximum thermal capacity, reaching values above 714 MWth; and second, a multi-week period where demand remains below the reactor's minimum operating threshold, set at 50% of its capacity, or 357 MWth.

4.1. First configuration: Only batteries

The first configuration includes three main units: the LFR-SMR, the industrial facility, and a lithium-ion battery system, as illustrated in Figure 3.

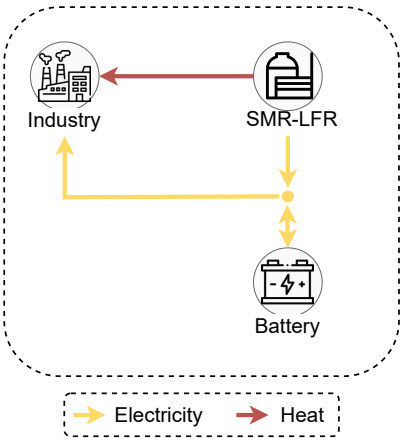

Figure 3: Configuration 1 with LFR-SMR, industrial facility, and lithium-ion battery system.

To ensure a continuous energy supply to the industrial facility throughout the year, we integrate a battery system as a secondary source of electricity. This battery relies on Nickel Manganese Cobalt (NMC) lithium-ion technology. This is a widely used technology characterised by its high energy density, which enables partial storage of the electricity generated by the reactor and facilitates the delivery of power to the industrial system when direct generation is insufficient or temporarily unavailable. In this configuration, the battery can only supply electricity demanded. This directly impacts the heat production, as in periods of energy deficit, there is a re-allocation of resources towards producing more heat and a greater reliance on the battery for electricity.

4.2. Second configuration: H_2-SOEC

In the second configuration, hydrogen production is integrated. Afterwards, this hydrogen can be used in a burner to provide an additional heat source for the industry, complementing the secondary electricity supply from Li-ion batteries. A representation is shown in Figure 4.

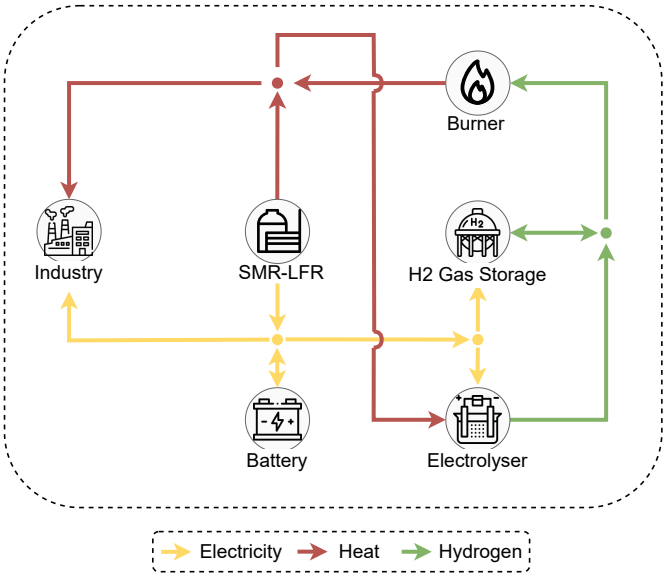

Figure 4: Configuration 2 building upon Configuration 1 with the integration of a hydrogen production and storage system

.

Hydrogen is produced using a high-temperature Solid Oxide Electrolyser Cell (SOEC). This electrolyser operates at elevated temperatures, allowing it to use not only the electricity produced by the LFR-SMR but also the heat generated by the reactor. This heat is utilised to produce high-temperature steam, which the SOEC leverages to achieve higher efficiencies compared to conventional electrolysers such as alkaline (AEC) and proton exchange membrane (PEM) systems [21].

In this configuration, the electricity generated by the LFR-SMR is used to supply the industrial facility, charge batteries, power the electrolyser, and operate compressors for hydrogen storage. The produced hydrogen can be stored as a gas at 500 bar and later burned to generate heat during peak consumption periods. Compressed hydrogen storage units are used to enhance flexibility between different units while ensuring the proper operation of the electrolysers. The hydrogen storage considered is a type 2 tank [22], capable of withstanding pressures of approximately 800 bar. It consists of a metal liner reinforced with a composite hoop winding.

4.3. Third configuration: NH_3-SOEC

Building upon the same strategy as in the previous configuration, this final configuration introduces ammonia alongside the existing battery and hydrogen components. This configuration in illustrated Figure 5.

Ammonia is synthesised from nitrogen and hydrogen, both produced by the SOEC. According to [23], this process relies on the combustion of a fraction of the hydrogen generated by steam electrolysis in the presence of air. The SOEC then acts as an oxygen separation membrane, using heat instead of electricity, eliminating the need for an air separation unit.

A Haber-Bosch process is used to synthesise ammonia by combining nitrogen and hydrogen under high pressure and high temperature with the help of a catalyst. Liquid ammonia tanks are included to provide flexibility between different subsystems. To store ammonia in its liquid form, it is kept at a temperature of -33°C [24]. A compressed nitrogen tank is used as a storage medium between the SOEC electrolyser and the ammonia synthesis process. Furthermore, the regasification unit converts liquid ammonia into its gaseous form, which is subsequently used to fuel the burner. Owing to ammonia's low flammability and high NOx emissions, it is blended with hydrogen prior to combustion in the burner [25].

5. Methodology

Previously, we have introduced the various configurations under study. In this section, we present the modelling framework used to represent these configurations. It determines the optimal capacities of the different storage and conversion units along with operational strategies for the entire system, enabling the SMR industry complex to operate off-grid continuously throughout the year.

This section begins with an overview of the optimisation framework, followed by the related assumptions. We then explain the technical constraints and assumptions specific to each technology, as described in Section 4.

5.1. Methodological framework

Our work is based on the methodology presented in [26] and [27], which employs the Graph-Based Optimisation Model Language (GBOML) as the optimisation framework. GBOML [28, 29] is a tool that allows one to model Mixed-Integer Linear Programs (MILPs) using hierarchical hypergraphs. In this framework, hypergraph nodes represent technologies, facilities, or processes, while hyperedges correspond to the commodity flows generated by these nodes. This approach

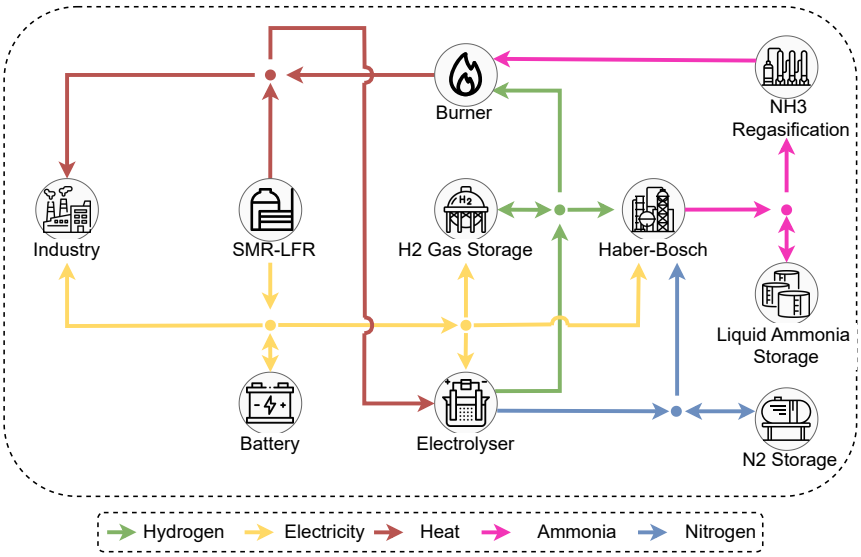

Figure 5: Configuration 3 extending configuration 1 and 2, with the addition of an ammonia production and storage system.

enables the hierarchical modelling of complex systems, where each node can encapsulate sub-nodes.

In this paper, we assume the immediate availability of assets following any investment, meaning that once an investment is made, the corresponding asset is considered directly available. All equations used are linear. We also make a perfect forecast hypothesis, implying that the entire energy demand curve is known in advance. The sizing of all components is performed through an optimisation framework that assumes that planning and investment decisions are made by a single entity. Transportation-related costs and infrastructure costs between and within each node are not modelled. Finally, the optimisation is carried out over a period of one year, with a resolution of fifteen minutes. The Weighted Average Cost of Capital (WACC) is fixed at 5 %.

5.2. Nodes

We detail the practical implementation of the various system nodes. A summary table presenting the projected economic parameters for each node in 2035, along with their respective lifespans, is provided in Appendix A.

Lead fast reactor

The lead fast reactor node illustrates the hierarchical modelling approach, grouping sub-nodes such as the reactor core, the thermal storage, the cooling tower, and the turbine representing the whole Rankine cycle used to produce electricity as illustrated in Figure 2.

The LFR-SMR is assumed to operate under optimal conditions, with no shutdowns occurring throughout its operation. Maintenance activities are not considered. Additionally, all sub-components of the LFR-SMR are described in detail in the following sections.

Reactor core

The operation of the reactor core is simplified in our model as a controllable heat source, constrained within a narrow temperature range between 495°C and 505°C. The core power output is bounded by a maximal heat output and by a minimal heat output. The maximum heat output taken into account is 714 MW. Load following is managed exclusively through reactivity control by inserting control rods. According to SCK-CEN experts, the reactor can operate between 50% and 100% of its capacity. Within this range, we consider a limitation on the number of complete load cycles. These constraints are based on the European Utilities Requirements (EUR) [30], which define the load-following capabilities expected of modern nuclear reactors operating within the European Union. Specifically, complete transitions from 50% to 100% of production capacity—and back—are restricted to a maximum of two cycles per day, five per week, and no more than 200 cycles per year.

Ramp-up and ramp-down constraints are taken into account. According to SCK-CEN experts, their demonstrator reactor is estimated to have a ramp rate varying between 16.75% and 67.00% per hour. Therefore, in our model, we set the ramp rate at the midpoint of this range, which is 41.90% for both ramp-up and ramp-down. Lastly, the effects of fuel ageing, namely the gradual degradation of nuclear fuel performance over time, are not taken into account in this study.

Thermal storage

As in the primary circuit, the temperature variation is limited to a maximum of 5°C. For simplification, the pressure, specific volume, and specific heat of molten salt are assumed to be constant, with the specific heat taken as 1.5 J/g K. Its temperature must always remain within a range to maintain a consistent (steady) efficiency of the Rankine cycle. Additionally, no heat losses are considered in the storage system.

Heat exchangers between the reactor core and the thermal storage system dimensions are assumed to be sufficient to ensure nominal power heat transfer.

Cooling tower

An efficiency of 75% is assumed for the cooling tower [31], implying that a maximum of 75% of the thermal energy entering the tower can be effectively dissipated. Furthermore, it is assumed that 1% of the generated electricity is consumed to operate auxiliary components such as pumps and fans [32].

Turbine

The selected Rankine cycle operates with superheated steam and is assumed to have a constant efficiency of 0.42 within the temperature range of 495-505 °C, based on assessments by SCK-CEN experts. This assumption is supported by the findings in [8].

Electrolyser

For the SOEC electrolysers, water flows are not explicitly modelled and are assumed to be freely available. Only energy balances are taken into account. In addition, a minimum operational load of 40% is considered, along with an efficiency of 81% [33], based on energy inputs (heat and electricity) and hydrogen as the output. It is also assumed that ramping constraints are negligible at the time resolution under consideration. Therefore, no ramping limitations are incorporated into the analysis.

Burner

The flow of hydrogen, as well as the hydrogen–ammonia mixture, is assumed to be converted into heat with an associated energy loss of 5%. The hydrogen–ammonia mixture is considered to contain a minimum 40% hydrogen by volume, as reported in [25].

Battery

The considered batteries have a self-discharge rate of 0.00004 per hour, and a charge/discharge rate of 0.959 [22].

Hydrogen storage

No hydrogen loss during storage is assumed, but electricity consumption is accounted for powering the compressors required to reach a pressure of 500 bars. A consumption of 5.56 kWhe/kg of hydrogen is considered. Moreover, the storage system is required to maintain a minimum hydrogen reserve, set at 5% of its total capacity [22].

Haber-bosch

The Haber-Bosch node includes a "hot standby" mode, which imposes a minimum operating threshold of 20%, with no ramp-up constraints. The overall efficiency is estimated at 82.3%, considering that 94.7% of the energy input originates from hydrogen, while the remaining 5.3% is provided by electricity [33]. In addition to the input flows of hydrogen and nitrogen, an electrical input is considered to power various auxiliary systems. Moreover, based on the modelling parameters provided by [33], ammonia at the output is assumed to be in liquid form. No external heat source is assumed, as the ammonia synthesis reaction is highly exothermic [33].

Liquid ammonia storage

A daily loss of 0.08% is assumed for the liquid ammonia tank due to interactions with ambient heat [34].

Ammonia regasification

Approximately 2% of the ammonia is considered necessary to meet its own heating requirements. Furthermore, it is assumed that the installation cost of such a unit [35] is comparable to that of a natural gas regasification unit.

Nitrogen storage

No storage losses are considered, and the temperature and pressure of nitrogen are assumed to be optimal throughout its path, from the SOEC output to the input of the Haber-Bosch unit.

6. Optimisation Results

Having established the three configurations involving the LFR-SMR and the industrial off-grid site, and after outlining the modelling and optimisation framework, we now proceed to analyse the results for each configuration.

To assess both the economic and technical performance of this off-grid scenario, we first examine the associated average costs, along with the installed capacities. Furthermore, to better understand the differences between configurations as well as to assess the performance of the LFR-SMR in an off-grid setting, we analyse the dynamic behaviours related to the optimal operational strategy in response to fluctuations in energy demand. Finally, a sensitivity analysis is conducted on several key parameters to enhance the robustness of the results.

Moreover, GBOML, the modelling tool introduced earlier in this study, is open-source and released under the MIT license, ensuring full reproducibility of the results. Access to the code and data associated with this work is given in Section 7.

6.1. Results

To improve clarity and readability, the results are structured into several focused sections. We begin with an examination of system costs, followed by a detailed analysis of the optimal capacities, including the amount of energy stored, battery and electrolyser sizes, as well as hydrogen and ammonia storage requirements. Finally, we conclude with an assessment of the dynamic behavior across the different system configurations.

Cost analysis

To evaluate the economic performance of these configurations, average costs have been estimated for each case. These average costs are determined by summing the annualised costs of each unit within the studied system (LFR-SMR, batteries,

electrolysers, storage units, ect.), along with the total heat demand for the industry over one year by using the following equation:

$$\text{Average Heat Cost} = \frac{\text{Total System Cost}}{\text{Total Heat Demand}} \tag{1}$$

Total heat demand is defined as the sum of the heat required to meet both the direct heat demand and the heat needed to produce electricity. This approach also enables one to derivate an average electricity cost by considering the efficiency of the turbine. A summary of the costs associated with the three configurations under study is provided in Table 1.

Average costs	Battery only	H_2-SOEC	NH_3-SOEC
Electricity [€/MWh]	92.3	59.6	58.7
Heat [€/MWh]	38.8	25.0	24.6

Table 1: Table of average costs per unit of electricity and heat production. The WACC considered is 5% and the LFR-SMR's CAPEX is estimated at 5,500 €/kW.

To provide a better perspective on these results, it is worth noting that, for all the configurations studied, the reactor capacity factor is approximately 0.8.

The costs associated with the hydrogen and ammonia configurations were found to be very similar. Their electricity cost is a little less than €60/MWh, while their heat cost is under €25/MWh. When considering only battery storage to ensure off-grid operation, the resulting average electricity and heat costs are €38.8/MWh and €92.3/MWh, respectively. These represent the highest costs among all configurations evaluated in this study, as shown in Table 1.

It is important to note that the majority of the costs associated with this system are linked to the LFR-SMR itself. Its cost remains constant across different configurations, as its capacity is fixed. The integration of production, storage, and conversion units for e-fuels accounts for only 4% to 5% of the total costs. By contrast, in the battery-only configuration, it represents 39%, as shown in Table 2.

Share in Total Cost	Battery only	H_2-SOEC	NH_3-SOEC
LFR-SMR [%]	61.0	94.8	96.1
Other Components [%]	39.0	5.2	3.9

Table 2: Proportion of storage and conversion unit costs in the total system cost.

The integration of ammonia resulted in a slight cost reduction compared to the hydrogen configuration. This is because storage primarily relies on liquid ammonia. This approach reduces the need for gaseous hydrogen storage, thereby offsetting the additional costs associated with the installation of a Haber-Bosch unit and a regasification unit. The difference in CAPEX and OPEX between the two types of storage (liquid ammonia and compressed hydrogen) can be seen in Table A.11.

Capacity installed

Let us compare the different capacities installed in each optimal configuration. Those are gathered in Table 3.

Installed Capacities	Battery only	H_2-SOEC	NH_3-SOEC
Electrolyser [MW]	-	2.9	4.1
Battery Storage [MWh]	2,763.6	33.7	6.9
Compressed Hydrogen Storage HHV [MWh]	-	16,448.4	3,875.4
Liquid Ammonia Storage Storage HHV [MWh]	-	-	15,450.0
Haber-Bosch [MW]	-	-	2.8
Regasification [MW]	-	-	45.9
Nitrogen Storage [kt]	-	-	0.0

Table 3: Comparative analysis of storage and conversion capacities across configurations.

The energy storage capacity (both in terms of electricity and molecules) is substantially higher in the synthetic fuel-based configurations compared to the battery-only one. Specifically, the total amount of energy stored in the form of hydrogen

and ammonia exceeds 15 GWh, whereas the battery-only configuration requires a battery capacity of around 2.8 GWh. To explain this difference, note that consuming one unit of electricity requires the production of $1/0.42 \approx 2.4$ units of heat. Storing one unit of electricity can thus be seen as an equivalent of storing 2.4 units of heat, explaining a large part of the change in energy stored. As the batteries are comparatively more expensive, the remaining difference is mainly linked to the cost and operation optimisation.

In configurations based on synthetic fuels, the majority of energy is stored in the form of hydrogen and ammonia, while their batteries provide only limited storage capacity. In the second configuration, which relies solely on hydrogen as an e-fuel, the battery capacity reaches 33.7 MWh. However, when ammonia is introduced as an additional fuel, the required battery capacity decreases significantly to 6.9 MWh. These variations in battery sizing are directly linked to the economic performance of the respective synthetic fuel supply chains. The integration of ammonia contributes to a notable reduction in overall system costs by alleviating the need for large-scale hydrogen storage, which, aside from the LFR-SMR itself, represents one of the main cost drivers in synthetic fuel-based configurations. In these two configurations, batteries play only a marginal role in meeting the total energy demand. The majority of the secondary energy supply is instead provided by the combustion of synthetic fuels in dedicated burners.

In terms of additional installed capacities, the hydrogen-based configuration includes an electrolyser with a capacity of 2.9 MW, while the configuration incorporating ammonia requires a higher electrolyser capacity of 4.1 MW. This increase can be attributed to the reduced overall efficiency of the energy conversion chain resulting from the integration of ammonia, particularly due to the energy requirements of the Haber-Bosch synthesis process, whose dedicated unit operates at a capacity of 2.8 MW. The fact that the electrolyser capacity in the ammonia configuration exceeds that of the Haber-Bosch unit suggests that hydrogen production remains significant even in the presence of ammonia. This can be explained by the need for hydrogen not only as a precursor in ammonia synthesis but also potentially as a complementary fuel during combustion, given the limitations of using ammonia alone as a direct energy carrier.

Volume storages

A substantial quantity of energy must be stored to ensure reliable off-grid operation, on the order of gigawatt-hours. This large energy storage requirement can translate into significant storage volumes, depending on the energy carrier used.

For example, in the hydrogen-based configuration, up to 16 GWh of hydrogen gas compressed at 500 bar must be stored. In comparison, the ammonia-based configuration requires considerably less hydrogen storage (less than 4 GWh) but still approximately 15.5 GWh in the form of liquid ammonia. These differences in storage highlight the significantly lower costs associated with ammonia storage compared to hydrogen, as detailed in Table A.11.

Accordingly, in terms of volume, the storage capacities of hydrogen and ammonia, with respective densities of 31 kg/m^3 (for storage at 500 bars) and 682 kg/m^3 (for liquid storage), are summarised in Table 4. In the hydrogen-based configuration, this corresponds to a storage capacity occupying approximately 13,380 m^3. By contrast, integrating ammonia reduces the hydrogen storage volume to about 3,160 m^3. When accounting for the additional ammonia storage, which requires roughly 3,630 m^3, the combined total storage space amounts to approximately 6,790 m^3.

Storage volume	Battery only	H_2-SOEC	NH_3-SOEC
Hydrogen storage [m^3]	-	13,380	3,160
Ammonia storage [m^3]	-	-	3,630
Battery storage [m^3]	3,500	43	9

Table 4: Table of storage capacities in volume. For compressed hydrogen at 500 bar and liquid ammonia at –33°C, the higher heating value (HHV) is considered for each conversion.

In the case of the first configuration, which involves only a battery system, the optimal capacity, previously mentioned as approximately 2.8 GWh, corresponds to a total volume of around 3,500 m^3, assuming an energy density of 800 Wh/L.

These large storage facilities pose significant safety risks, particularly because hydrogen is highly susceptible to leaks and is extremely flammable [36]. Ammonia similarly presents serious health and safety concerns, while batteries carry the risk of fire and/or explosion. Although a comprehensive risk assessment is essential to address these issues, it falls beyond the scope of the present study.

Dynamics of the proposed configurations

We begin by examining how the system responds to varying demand levels throughout the year. To illustrate this dynamic, Figure 6 depicts the total industrial heat demand, including both the heat required for electricity generation and direct industrial heat consumption, as well as the heat produced by the LFR-SMR (the heat output from the thermal storage). The operational range of the LFR-SMR is clearly visible, constrained by its maximum capacity of 714 MWth and its minimum operational limit, set at 50% of its capacity, 357 MWth (Subsection 5.2). When demand exceeds this range, such as during winter months, where peak requirements surpass the reactor's maximum output, the system must rely on previously stored energy to meet the demand. Conversely, during summer periods when heat demand falls below the reactor's minimum output, the system must either dissipate excess heat and/or store surplus energy. A clear seasonal effect

can therefore be observed. For the rest of the year, the model follows demand closely, requiring little to no use of storage and conversion systems such as batteries and electrolysers.

Figure 6: Representation of heat demand and the heat required for electricity demand over a full year, as well as the annual heat production of the LFR-SMR. Representation taken from configuration H_2-SOEC.

In the battery-only configuration, which lacks any additional heat source, winter peak energy demands are met through electricity demand. This allows heat to be preserved, as there is no need to generate additional electricity for demand, which is instead supplied by the batteries.

Figure 7 illustrates the system's capability to accurately track fluctuations in demand using the ammonia configuration (the hydrogen configuration behaves similarly).

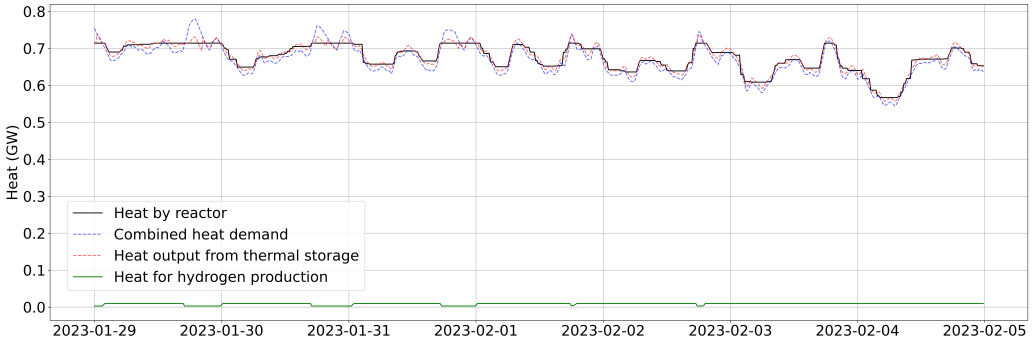

Figure 7: Representation of heat management during a winter week (Configuration NH3-SOEC).

The thermal output of the reactor (heat by reactor) shows limited flexibility due to ramping constraints, which prevent it from accurately tracking the heat demand (combined heat demand). In contrast, the heat delivered by the secondary circuit (heat output from thermal storage) follows the demand more closely. The secondary circuit does not face ramping limitations but must ensure that its temperature variation does not exceed 5°C (see Subsection 5.2). As a result, the heat output from the thermal storage is better aligned with the demand. Furthermore, a slight surplus of heat from the secondary circuit is also observed, allowing for a near-continuous hydrogen production outside of peak consumption periods.

At several moments, the total heat demand exceeds the reactor's maximum capacity (set at 714 MW), requiring the activation of a secondary heat source, the burner, which operates through the combustion of e-fuels. As shown in Figure 8, the burner is primarily used during the winter months, when peak consumption occurs. A similar dynamic is observed in the configuration relying solely on a battery as a secondary energy source.

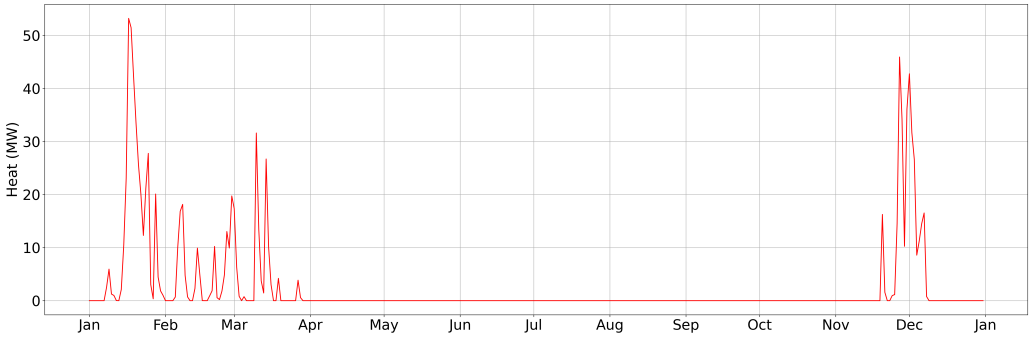

Figure 8: Representation of heat production by the burner (Configuration H_2-SOEC, similar to NH_3-SOEC).

The total amount of heat produced by the burner in the two synthetic fuel-based configurations is presented in Table 5.

This corresponds to approximately 25 GWh of heat required to ensure a sufficient energy supply for the industry. In contrast, the battery-only configuration delivers slightly more than 11 GWh of electricity over the course of the year. On average, these supplementary energy sources contribute less than 1% of the industry's total energy demand, underscoring the extent to which the LFR-SMR, with its thermal storage, is largely capable of meeting the industry's demand on its own.

	Battery only	H_2-SOEC	NH_3-SOEC
Heat by Burner [GWh]	-	21.3	25.9
Heat rejected [GWh]	7.0	5.5	5.1

Table 5: Total heat produced through the burner and high-quality heat dissipated through the cooling tower over the year.

During the summer period, the reactor must evacuate excess heat, as illustrated in Figure 6. A substantial portion of this heat is discharged via the cooling tower. In the synthetic fuel-based configurations, approximately 5 GWh of high-grade heat is evacuated (Table 5), whereas this value increases to about 7.0 GWh in the battery-only case, most of which is released over a concentrated 15-day period in summer. This heat originates from the secondary circuit (thermal storage) and is considered high quality, as it can directly meet industrial heat demand or support electrolyser operation in e-fuel configurations.

In parallel, the cooling tower handles the removal of low-grade residual heat from the turbine. This quantity is considerably greater, reaching nearly 970 GWh per year in the synthetic-fuel configurations and approximately 920 GWh in the battery-only case. Since the industrial electricity demand remains constant across all configurations, these differences are primarily attributable to variations in the energy conversion efficiencies specific to each configuration.

6.2. Sensitivity analysis

Since the LFR-SMR represents the largest cost component in each model (see Table 2), and given the uncertainty surrounding its capital expenditure (CAPEX) and investment costs, we conducted a sensitivity analysis on both the CAPEX and the weighted average cost of capital (WACC). Specifically, we examine two additional CAPEX values: €4,000/kW and €7,000/kW, alongside the originally selected CAPEX of €5,500/kW, which is analysed with a WACC of 7%.

With an off-grid situation, the LFR-SMR must be capable of, at least partially, operating in load-following mode. With a current ramping rate of 41.90% per hour (see Subsection 5.2), which allows for power adjustments based on demand, we analyse an additional scenario where ramping is limited to 1% per hour. The objective is to assess the impact of limiting the reactor's ability to adapt to demand fluctuations on the cost, conversion and storage units.

Finally, considering the economic advantage of using e-fuels to enable off-grid operation, an additional analysis is performed to assess the inclusion of alternative electrolyser technologies, namely Alkaline electrolysers (AEC) and Proton Exchange Membrane electrolysers (PEM).

Sensitivity on CAPEX & WACC

Reducing the LFR-SMR CAPEX to €4,000/kW (≈ -30% compared to the baseline) leads to a decrease in the average electricity and heat costs to approximately €48/MWh and €20/MWh, respectively (Table 6) for the two synthetic-fuels-based configurations. This represents a 20% reduction in energy costs compared to the baseline scenario (Table 1).

For the battery-only approach, this leads to average heat and electricity costs of €34/MWh and €81/MWh, respectively, representing a decrease of approximately 12%.

Average costs	Battery only	H_2-SOEC	NH_3-SOEC
	CAPEX 5,500€/kW with WACC 5%		
Electricity [€/MWh]	92.3	59.6	58.7
Heat [€/MWh]	38.8	25.0	24.6
	CAPEX 4,000€/kW with WACC 5%		
Electricity [€/MWh]	80.8	48.1	47.2
Heat [€/MWh]	33.9	20.2	19.8
	CAPEX 7,000€/kW with WACC 5%		
Electricity [€/MWh]	103.8	71.1	70.2
Heat [€/MWh]	43.6	29.9	29.5
	CAPEX 5,500€/kW with WACC 7%		
Electricity [€/MWh]	107.0	74.3	73.4
Heat [€/MWh]	44.9	31.2	30.8

Table 6: Sensitivity analysis on the WACC and CAPEX of the LFR-SMR.

Conversely, an increase in CAPEX to €7,000/kW (i.e., approximately 30% above the baseline) results in higher electricity and heat generation costs. For hydrogen- an ammonia-based configurations, the average costs rise to approximately €70/MWh for electricity and €30/MWh for heat. In the battery-only configuration, these costs reach €104/MWh and €44/MWh, respectively. This represents an increase of approximately 15% and 12% in total energy costs for the synthetic fuels and battery-only configurations, respectively.

Similarly, when the WACC is increased to 7%, the average electricity and heat costs rise to €73/MWh and €30/MWh, and €107/MWh and €45/MWh, respectively, for the three configurations analysed.

Since these changes only apply to the LFR-SMR, which is fixed at 300 MWe, there is no impact on other units such as electrolysers, batteries, etc.

Sensitivity on ramping

When the reactor's ability to follow demand is constrained by a ramping rate limited to 1% of its nominal power per hour, both the amount of heat rejected by the cooling tower and the heat produced by the burner increase.

A slight increase in burner usage is observed, resulting from the reactor's limited ability to modulate power output rapidly in response to variations in energy demand. This increase amounts to approximately 9% for the hydrogen configuration and 4% for the ammonia configuration. Due to this more limited flexibility, the system relies more on the cooling tower to accommodate demand fluctuations. The same behaviour is observed in the battery-only configuration.

	Battery only	H_2-SOEC	NH_3-SOEC
Heat by Burner [GWh]	-	23.3	26.9
Heat rejected [GWh]	59.2	49.51	80.0

Table 7: Total heat produced through the burner and high-quality heat dissipated through the cooling tower over the year. Configurations with a 1% per hour ramping constraint for the LFR-SMR.

Indeed, to better match production with consumption, the reactor tends to overproduce and dissipate excess heat from the secondary circuit in the cooling tower, ensuring a more responsive energy supply. The annual heat dissipation reaches approximately 50 GWh and 80 GWh for the hydrogen and ammonia configurations, respectively, and around 60 GWh when using batteries alone (see Table 7).

Although the reactor's ramping capacity decreases significantly, the use of heat from the burner and the heat evacuated by the cooling tower remains marginal compared to the total heat (and electricity) generated by the reactor, which is directly used by the industry without passing through conversion or storage units. Indeed, with 4,000 GWh, of which 85% is dedicated to the industry's heat demand, the amount of heat supplied through the burner remains very low.

No significant differences are observed in the capacities of the storage and conversion units, nor in the capacity of the battery for the battery-only configuration. Since the demand remains the same, the winter peaks remain unchanged, and therefore the units remain the same, sized for these peaks. Moreover, there is no significant change in the reactor's capacity factor, and therefore the average electricity and heat costs remain comparable to those of the previous configuration.

Sensitivity on electrolysers

The previous results have shown that the use of e-fuels leads to a significant cost reduction compared to the configuration relying solely on batteries. To assess whether alternative electrolyser technologies could offer further advantages, two widely used options were selected: Proton Exchange Membrane (PEM) and Alkaline electrolysers (AEC), both used for hydrogen production.

However, unlike SOEC, these technologies cannot directly produce nitrogen, which is required for subsequent ammonia synthesis. They would thus require an additional air separation unit, an element we chose not to include in order to limit the number of configurations considered. The analysis is therefore restricted to hydrogen configurations.

A technical comparison of the three electrolyser types is presented in Table 8, while the costs associated with each technology are detailed in Appendix A.

Electrolyser	Minimum capacities	Lifetime	Efficiency
AEC	15%	8 yr	69%
PEM	5%	6 yr	63%
SOEC	40%	3 yr	81%

Table 8: Parameters for modelling electrolysers [33], with efficiency based on energy input (electricity and heat for SOEC) relative to hydrogen production, considering HHV.

When switching to AEC and PEM electrolysers for hydrogen production, and applying the cost calculation given by Equation 1, we obtain average electricity and heat costs of approximately €59/MWh and €25/MWh, respectively. These

values, as shown in Table 9, are comparable to those obtained using an SOEC electrolyser. Indeed, since the cost of the LFR-SMR already constitutes the vast majority of total expenses, the influence of the electrolyser type on overall costs remains relatively minor.

Average costs	H_2-AEC	H_2-PEM	H_2-SOEC
Electricity [€/MWh]	58.8	59.3	59.6
Heat [€/MWh]	24.7	24.9	25.0

Table 9: Table of average costs per unit of electricity and heat production. The WACC considered is 5% and the LFR-SMR's CAPEX is estimated at 5,500 €/kW.

However, differences in installed capacities are observed among the electrolyser technologies, as presented in Table 10. Specifically, the SOEC technology requires the lowest installed capacity for hydrogen production, at 2.9 MW. In contrast, the AEC technology demands a significantly higher installed capacity of 13.1 MW, while the PEM electrolyser requires 10.0 MW. These differences can be attributed to variations in both the efficiency of each electrolyser type (see Table 8) and their respective operational expenditures (OPEX, detailed in Table A.11). Higher operating costs lead to less frequent utilisation, thereby influencing the required installed capacity.

Employing SOEC electrolysers (which are associated with higher OPEX) promote a more continuous hydrogen production, unlike PEM and AEC electrolysers, which operate at specific times. These differences in dynamics can be observed in Appendix B, which presents graphs of the total heat demand and heat production from the LFR-SMR. We observe a nearly continuous overproduction by the reactor to generate the necessary hydrogen when it is produced by a SOEC, whereas the AEC and PEM models exhibit a more responsive, demand-tracking behaviour.

This enhanced operational flexibility contributes to a significant reduction in required hydrogen storage, as seen in Table 10. Specifically, the volume of compressed hydrogen storage drops to approximately 10 GWh, compared to 16 GWh in the SOEC case.

Installed Capacities	H_2-AEC	H_2-PEM	H_2-SOEC
Electrolyser [MW]	13.1	10.0	2.9
Compressed Hydrogen Storage HHV [MWh]	9,847.5	10,634.6	16,448.4

Table 10: Comparisons of electrolysers and compressed hydrogen storage in hydrogen configurations

7. Conclusion

This study has investigated the deployment of a specific type of SMR to power an energy-intensive industrial site operating off-grid for a full year. The SMR is based on lead-cooled fast reactor technology and is coupled with a molten salt thermal storage unit and a cooling tower, which enables more flexible heat delivery. A key challenge in this context arises from the strong seasonal variability of the industry's energy demand. The LFR-SMR alone cannot meet peak consumption demand during the winter months and tends to overproduce during several days in the summer. This mismatch requires the deployment of complementary energy conversion and storage units, both to store surplus energy, and to provide it during periods of deficit, thereby ensuring uninterrupted industrial operations.

To address this challenge, three configurations were evaluated using real electricity and heat consumption data from an operational chemical plant in Belgium. Each configuration builds incrementally on the previous one by integrating additional energy storage vectors. The first configuration includes battery storage; the second adds hydrogen to the battery system; and the third further incorporates ammonia as an additional energy vector. In the battery-only configuration, the industry can be supplied directly with electricity from the storage system. In contrast, the two other configurations also allow the LFR-SMR to produce and store high-energy-density molecules (hydrogen and ammonia) that can later be burned to meet the thermal demand of the industrial process. The sizing of these complementary energy conversion and storage units into the SMR-industry system was guided by optimisation models developed to determine the optimal sizing and operational strategies over a one-year horizon, with a temporal resolution of 15 minutes. Furthermore, a sensitivity analysis was conducted on technical and economic parameters of the LFR-SMR, including its CAPEX, WACC, and ramping capabilities. In addition, different electrolyser technologies were evaluated for hydrogen production.

Three main insights emerge from this study.

First, using e-fuels to cover winter demand peaks proves to be more cost-effective than relying solely on battery storage. Based on the baseline assumptions and the cost estimation methodology applied in this study, configurations integrating e-fuels show similar overall costs, with average heat costs around €25/MWh and electricity costs around €60/MWh. In these configurations, the contribution of complementary conversion and storage units represents approximately 5% of the

total system cost, with a slight advantage observed when ammonia is included (4%). In contrast, when only batteries are used, this share increases significantly, reaching up to 40% of the total system cost.

Second, the LFR-SMR, when operating within its nominal power range, i.e., outside winter peak demand periods and summer overproduction episodes, and coupled with thermal energy storage (molten salt) and a cooling tower, is capable of following the demand curve without the need for additional units, even when the reactor has a limited ramping rate capability (1% per hour). This highlights the system's ability to operate autonomously for the vast majority of the year.

Third, the high annual energy demand of the industrial site leads to substantial storage requirements, on the order of gigawatt-hours. This translates to large-scale storage needs for hydrogen and ammonia, as well as a considerable volume of batteries, which remains exceptional in scale as at the time of publication (2025). While such storage appears technically feasible within the context of an industrial site, it raises significant safety and logistical challenges that must be carefully addressed in future work.

While the present work focuses on a fully off-grid configuration, future studies should also consider hybrid scenarios, in which the site operates independently only during periods of grid unavailability. The modelling framework developed in this study can be readily extended to such cases by introducing energy grids and appropriate operational constraints to ensure full load coverage during disruption periods. Partial integration with the grid (assuming zero connection costs) would likely reduce overall system costs. Access to the grid might alleviate the need to oversize storage and conversion units for year-round operation, particularly during periods of peak winter demand, while simultaneously enabling a higher capacity factor for the SMR reactor. Consequently, the cost estimates presented in this study can be interpreted as an upper bound for heat and electricity generation for systems where an LFR-SMR is deployed to enhance industrial autonomy from the grid.

Glossary

- AEC: Alkaline Electrolyser
- CAPEX: Capital Expenditure
- GBOML: Graph-Based Optimisation Modelling Language
- HHV: Higher Heating Value
- LCOE: Levelised Cost of Energy
- LFR: Lead-cooled Fast Reactor
- MOX: Mixed Oxide
- OPEX: Operating Expenditure
- PEM: Proton Exchange Membrane
- SCK-CEN: Studiecentrum voor Kernenergie ou Centre d'Etude de l'Energie Nucléaire
- SMR: Small Modular Reactor
- SOEC: Solid Oxide electrolyser Cell
- WACC: Weighted Average Cost of Capital

Competing interests

The authors declare no competing interests.

Acknowledgements

This work was carried out in collaboration with SCK-CEN, whose valuable discussions and scientific exchanges are acknowledged. The authors thank Jocelyn Mbenoun from the University of Liège for his insightful contribution to the conclusion section. Antoine Larbanois and Guillaume Derval acknowledge the financial support received from the Belgian authorities through the SCK-CEN for the LFR-SMR research.

Declaration of Generative AI and AI-assisted technologies in the writing process

During the preparation of this work, the author(s) used ChatGPT in order to correct the readability, grammar, and spelling of the writing. After using this tool/service, the authors reviewed and edited the content as needed and take full responsibility for the content of the publication.

Code and Data Availability

We emphasise that the code and data underlying this study have been released as open source [37]: https://doi.org/10.5281/zenodo.16403205

References

[1] Elia, Electricity scenarios for electricity Belgium towards 2050, 2017. URL: https://www.elia.be/-/media/project/elia/elia-site/electricity-market-and-system---document-library/adequacy---studies/2017/20171114_electricity-scenarios-for-belgium-towards-2050.pdf.

[2] Federal Planning Bureau, Perspectives énergétiques de la Belgique à politique annoncée, 2024. URL: https://www.plan.be/sites/default/files/documents/FOR_Energy2024_13004_FR.pdf.

[3] SCK-CEN, Leaders in heavy liquid metal technology join forces for deploying lead-cooled small modular reactors — sckcen.be, 2023. URL: https://www.sckcen.be/en/news/leaders-heavy-liquid-metal-technology-join-forces-deploying-lead-cooled-small-modular-reactors, [Accessed 2024-07-25].

[4] C. A. Lloyd, T. Roulstone, R. E. Lyons, Transport, constructability, and economic advantages of SMR modularization, Progress in Nuclear Energy 134 (2021) 103672. doi:https://doi.org/10.1016/j.pnucene.2021.103672.

[5] Ingersoll, D. Tilson, Passive safety features for small modular reactors, World Scientific, 2011, p. 113–121. doi:https://doi.org/10.1142/9789814365932_0012.

[6] M. Vanatta, D. Patel, T. Allen, D. Cooper, M. T. Craig, Techno economic analysis of small modular reactors decarbonizing industrial process heat, Joule 7 (2023) 713–737. doi:https://doi.org/10.1016/j.joule.2023.03.009.

[7] G. Locatelli, A. Fiordaliso, S. Boarin, M. E. Ricotti, Cogeneration: An option to facilitate load following in small modular reactors, Progress in Nuclear Energy 97 (2017) 153–161. doi:https://doi.org/10.1016/j.pnucene.2016.12.012.

[8] S. M. Kissick, H. Wang, A comparative study of alternative power cycles for small modular reactors, Energy Conversion and Management 247 (2021) 114734. doi:https://doi.org/10.1016/j.enconman.2021.114734.

[9] T. Wakabayashi, Concept of a fast breeder reactor to transmute MAs and LLFPs, Scientific Reports 11 (2021). doi:https://doi.org/10.1038/s41598-021-01986-w.

[10] K. Ikeda, T. Kawakita, Y. Ohkubo, High level radio-active wastes reduction through fast reactor, Progress in Nuclear Energy 37 (2000) 163–168. doi:https://doi.org/10.1016/S0149-1970(00)00042-1.

[11] Bloomberg, Germany warns of industry shutdown if Russian gas stops flowing, 2023. URL: https://www.bloomberg.com/news/articles/2023-06-12/germany-warns-of-industry-shutdown-if-russian-gas-stops-flowing, [Accessed 2025-06-30].

[12] Reuters, Power begins to return after huge outage hits spain and portugal, 2025. URL: https://www.reuters.com/world/europe/large-parts-spain-portugal-hit-by-power-outage-2025-04-28/, [Accessed 2025-06-30].

[13] Wojtaszek, D. Tadeusz, Potential off-grid markets for SMRs in Canada, CNL Nuclear Review 8 (2017) 87–96.

[14] J. Wallenius, S. Qvist, I. Mickus, S. Bortot, P. Szakalos, J. Ejenstam, Design of sealer, a very small lead-cooled reactor for commercial power production in off-grid applications, Nuclear Engineering and Design 338 (2018) 23–33. doi:https://doi.org/10.1016/j.nucengdes.2018.07.031.

[15] G. Locatelli, S. Boarin, A. Fiordaliso, M. E. Ricotti, Load following of small modular reactors (SMR) by cogeneration of hydrogen: A techno-economic analysis, Energy 148 (2018) 494–505. doi:https://doi.org/10.1016/j.energy.2018.01.041.

[16] G. Locatelli, S. Boarin, F. Pellegrino, M. E. Ricotti, Load following with small modular reactors (SMR): A real options analysis, Energy 80 (2015) 41–54. doi:https://doi.org/10.1016/j.energy.2014.11.040.

[17] Q. Ma, X. Wei, J. Qing, W. Jiao, R. Xu, Load following of SMR based on a flexible load, Energy 183 (2019) 733–746. doi:https://doi.org/10.1016/j.energy.2019.06.172.

[18] S. Ashoori, I. D. Gates, Small modular nuclear reactors: A pathway to cost savings and environmental progress in SAGD operations, Next Energy 4 (2024) 100128. doi:https://doi.org/10.1016/j.nxener.2024.100128.

[19] N. Van Hee, H. Peremans, P. Nimmegeers, Economic potential and barriers of small modular reactors in Europe, Renewable and Sustainable Energy Reviews 203 (2024) 114743. doi:https://doi.org/10.1016/j.rser.2024.114743.

[20] SCK-CEN, Lead-cooled fast reactor: SMR, 2025. URL: https://www.sckcen.be/en/expertises/nuclear-systems/lead-cooled-fast-reactor-belgium/small-modular-reactor-smr, [Accessed 2025-05-15].

[21] F. van Berkel, H. van 't Noordende, M. Stodolny, Next level solid oxide electrolysis: Upscaling potential and techno-economic evaluation for three industrial use cases, Technical Report, Institute for Sustainable Process Technology (ISPT), 2023. URL: https://ispt.eu/publications/next-level-solid-oxide-electrolysis/.

[22] Danish Energy Agency, Technology data for energy storage, 2023. URL: https://ens.dk/en/analyses-and-statistics/technology-catalogues, [Accessed 2024-07-25].

[23] J. B. Hansen, P. V. Hendriksen, The SOEC4NH3 project. Production and use of ammonia by solid oxide cells, ECS Transactions 91 (2019) 2455–2465. doi:https://doi.org/10.1149/09101.2455ecst.

[24] E. R. Morgan, Techno-economic feasibility study of ammonia plants powered by offshore wind, University of Massachusetts Amherst 385 (2013) 403. doi:https://doi.org/10.7275/11kt-3f59.

[25] W. S. Chai, Y. Bao, P. Jin, G. Tang, L. Zhou, A review on ammonia, ammonia-hydrogen and ammonia-methane fuels, Renewable and Sustainable Energy Reviews 147 (2021) 111254. doi:https://doi.org/10.1016/j.rser.2021.111254.

[26] M. Berger, D. Radu, G. Detienne, T. Deschuyteneer, A. Richel, D. Ernst, Remote renewable hubs for carbon-neutral synthetic fuel production, Frontiers in Energy Research 9 (2021). doi:https://doi.org/10.3389/fenrg.2021.671279.

[27] M. Fonder, P. Counotte, V. Dachet, J. de Séjournet, D. Ernst, Synthetic methane for closing the carbon loop: Comparative study of three carbon sources for remote carbon-neutral fuel synthetization, Applied Energy 358 (2024) 122606. doi:https://doi.org/10.1016/j.apenergy.2023.122606.

[28] B. Miftari, M. Berger, H. Djelassi, D. Ernst, GBOML: Graph-based optimization modeling language, Journal of Open Source Software 7 (2022) 4158. doi:https://doi.org/10.21105/joss.04158.

[29] B. Miftari, M. Berger, G. Derval, Q. Louveaux, D. Ernst, GBOML: A structure-exploiting optimization modelling language in Python, Optimization Methods and Software (2023). doi:10.1080/10556788.2023.2246169.

[30] OECD, Nuclear Energy Agency, Technical and Economic Aspects of Load Following with Nuclear Power Plants, OECD, 2021. doi:https://doi.org/10.1787/29e7df00-en.

[31] M. Choi, L. Glicksman, Computer optimization of dry and wet/dry cooling tower systems for large fossil and nuclear power plants, Technical Report / M.S. thesis MIT-EL-79-034, MIT Energy Laboratory, 1979. URL: https://dspace.mit.edu/handle/1721.1/35197.

[32] World Nuclear Association, World nuclear association: Cooling power plants, 2020. URL: https://world-nuclear.org/information-library/current-and-future-generation/cooling-power-plants, [Accessed 2025-02-15].

[33] Danish Energy Agency, Technology data for renewable fuels, 2023. URL: https://ens.dk/en/analyses-and-statistics/technology-catalogues, [Accessed 2024-07-26].

[34] DNV GL, Study on the import of liquid renewable energy: Technology cost assessment, 2020. URL: https://www.gie.eu/wp-content/uploads/filr/2598/DNV-GL_Study-GLE-Technologies-and-costs-analysis-on-imports-of-liquid-renewable-energy.pdf, [Accessed 2024-07-25].

[35] J. Pospíšil, P. Charvát, O. Arsenyeva, L. Klimeš, M. Špiláček, J. J. Klemeš, Energy demand of liquefaction and regasification of natural gas and the potential of LNG for operative thermal energy storage, Renewable and Sustainable Energy Reviews 99 (2019) 1–15. doi:https:

//doi.org/10.1016/j.rser.2018.09.027.
[36] S. T. Le, T. N. Nguyen, S. Linforth, T. D. Ngo, Safety investigation of hydrogen energy storage systems using quantitative risk assessment, International Journal of Hydrogen Energy 48 (2023) 2861–2875. doi:https://doi.org/10.1016/j.ijhydene.2022.10.082.
[37] A. Larbanois, Lead-cooled fast reactor SMR integration: An off- grid study case based on a real-life demand (code & data), 2025. URL: https://doi.org/10.5281/zenodo.16403205. doi:10.5281/zenodo.16403205.
[38] Danish Energy Agency, Technology data for industrial process heat— ens.dk, 2025. URL: https://ens.dk/en/analyses-and-statistics/technology-catalogues, [Accessed 2025-04-10].

A. Economic parameters used to model nodes

	CAPEX	FOM	VOM	Lifetime
SMR - Lead cooled Fast Reactor Assumed	5,500.0 M€/GW	50 M€/GW-yr	0.0 M€/GWh	60 yr
Battery storage [22]	210.0 M€/GW 185.0 M€/GWh	0.5 M€/GW-yr 0.0 M€/GWh-yr	0.0 M€/GWh 0.0018 M€/GWh	10 yr
H_2 Storage [22]	90.0 M€/kt_{H_2} 0.10 M€/kt_{H_2}/h	2.25 M€/kt_{H_2}-yr 0.001 M€/kt_{H_2}/h-yr	0.0 M€/kt_{H_2} 0.0 M€/kt_{H_2}	25 yr
Alkaline electrolyser (AEC) [33]	675.0 M€/GW_{el}	33 M€/GW_{el}-yr	0.0 M€/GWh	8 yr
Proton exchange membrane (PEM) [33]	950.0 M€/GW_{el}	40 M€/GW_{el}-yr	0.0 M€/GWh	6 yr
Solid oxide electrolyser cell (SOEC) [33]	1,250.0 M€/GW_{el}	150 M€/GW_{el}-yr	0.0 M€/GWh	5 yr
Burner [38]	36.0 M€/GW	0.0 M€/GW-yr	0.0 M€/GWh	25 yr
Haber-Bosch [33]	6,825.0 M€/kt_{NH_3}/h	204.75 M€/kt_{NH_3}/h-yr	0.000105 M€/kt_{NH3}	30 yr
Liquefied NH_3 storage [33] [24]	0.867 M€/kt_{NH_3} 0.10 M€/kt_{NH_3}/h	0.01735 M€/kt_{NH_3}-yr 0.001 M€/kt_{NH_3}/h-yr	0.0 M€/kt_{NH_3} 0.0 M€/kt_{NH_3}	30 yr
LNH_3 regasification Assumed	1,248.3 M€/kt_{LNH_3}/h	29.97 M€/kt_{LNH_3}/h-yr	0.0 M€/kt_{LNH3}	30 yr
N_2 storage Assumed	45.0 M€/kt_{N_2}	2.25 M€/kt_{N_2}-yr	0.0 M€/kt_{N_2}	30 yr

Table A.11: Economical parameters used for modelling conversion nodes (2035 estimates).

B. Additional representations

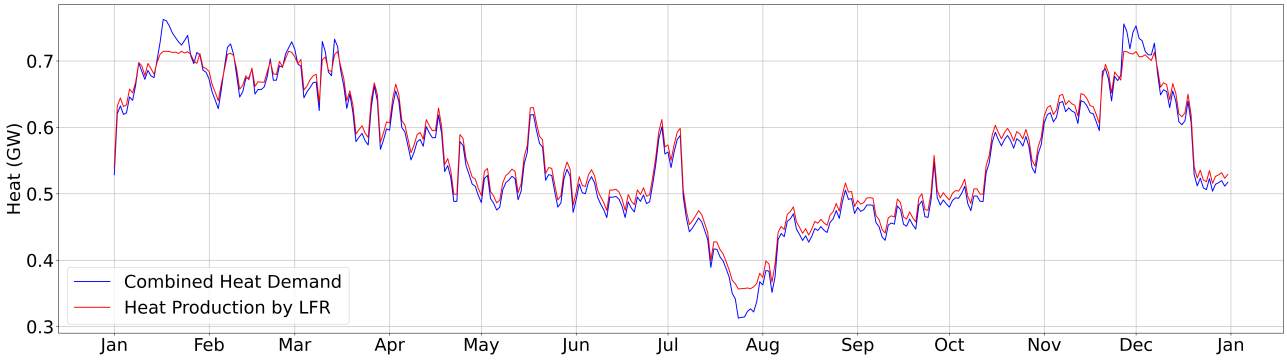

Figure B.9: Representation of heat demand and the heat required for electricity demand, as well as the heat production of the reactor. Representation taken from model NH3-SOEC (similar to H2-SOEC).

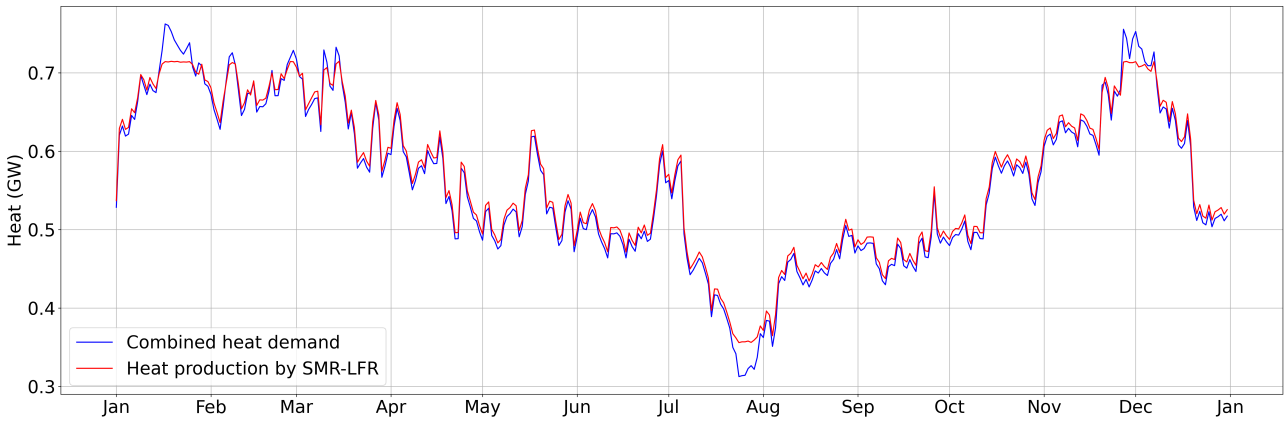

Figure B.10: Representation of heat demand and the heat required for electricity demand, as well as the heat production of the reactor. Representation taken from model H2-AEC (similar to H2-PEM).